XLVI CILAMCE
VITÓRIA - ES - BRAZIL - 2025
XLVI IBERO-LATIN AMERICAN CONGRESS ON COMPUTATIONAL METHODS IN ENGENEERING

A Goal-Oriented Error Estimator for Stress Intensity Factors in G/XFEM

Gabriela M. Fonseca[1], Rafael M. Lins[2], Felício B. Barros[1]

[1]*Graduate Program in Structural Engineering (PROPEEs), Federal University of Minas Gerais (UFMG)*
Avenida Antônio Carlos, 31270-901, Belo Horizonte, Brazil
gmarinhofonseca@gmail.com, felicio@dees.ufmg.br
[2]*Aeronautics and Aerospace Engineering Division (IEA-E), Aeronautics Institute of Technology (ITA)*
Praça Marechal Eduardo Gomes, 12228-900, São José dos Campos, Brazil
mlins@ita.br

Abstract. This work presents a goal-oriented error estimator specifically developed to quantify the error in the Stress Intensity Factor (SIF) for problems in Linear Elastic Fracture Mechanics. The estimator is formulated within the framework of the Generalized/eXtended Finite Element Method (G/XFEM), a widely used numerical technique for solving problems involving discontinuities and singularities. The analysis focuses on two-dimensional cases, with the SIF computed using the Interaction Integral — an energy-based method expressed as a domain integral. To estimate the error, a dual problem is constructed using the same discretization space as the primal problem. The estimated SIF error is then derived from the energy norm errors of both problems. For the energy norm estimation, the ZZ-BD recovery-based estimator is employed. This technique builds a recovered stress field using special enrichment functions and solves block-diagonal systems of equations, ensuring both computational efficiency and high accuracy. Numerical results for a mixed-mode fracture problem confirm the effectiveness of the proposed strategy, resulting in effectivity indices close to unity. Furthermore, the element-wise distribution of the estimated error closely reflects the characteristics of the Interaction Integral. All simulations were performed using INSANE, an open-source platform developed at the Department of Structural Engineering of the Federal University of Minas Gerais.

Keywords: Error estimator, Stress intensity factor, Generalized Finite Element Method, Recovered stresses, Fracture mechanics.

1 Introduction

The Generalized Finite Element Method (G/XFEM) [1] [2, 3] has established itself as a robust technique in Computational Mechanics, especially for the simulation of fracture problems. Although G/XFEM is not strictly a mesh-free method, it adopts a similar philosophy by enriching the numerical approximation with special functions (enrichment functions), which decreases the dependency on the finite element mesh. This enrichment strategy provides greater flexibility in mesh design, allowing the mesh to better adapt and capture local phenomena such as cracks that do not coincide with element boundaries.

The study of errors in approximate solutions has been extensively addressed in G/XFEM literature over the past decades [4]. Besides *a priori* error estimates, which serve as the theoretical foundation for the method, several *a posteriori* error estimators have been developed. These estimators rely on information derived directly from the approximate solution. In fracture mechanics applications, most existing estimators use gradient recovery procedures, where a recovered stress field is employed to quantify the error. For example, Lins et al. [5] proposed an estimator in this category that modifies the system matrix to a block-diagonal form, thereby improving computational efficiency.

Within this context, the present work introduces a goal-oriented error estimator tailored specifically to the error in the Stress Intensity Factor (SIF) obtained via G/XFEM. Using the Interaction Integral method [6] for SIF extraction, a dual problem linked to the quantity of interest is defined. Then, employing estimated errors in the energy norm for both primal and dual problems – calculated through the aforementioned ZZ-BD technique – an error estimate for the SIF is derived. The proposed methodology is applied to a two-dimensional fracture mechan-

[1] In this work, G/XFEM and the Extended Finite Element Method (XFEM) are treated as equivalent formulations, as discussed in [1].

ics problem under mixed-mode crack opening. This research was conducted using the computational platform *INSANE* (*IN*teractive *S*tructural *AN*alysis *E*nvironment), an open-source software developed at the Department of Structural Engineering of the Federal University of Minas Gerais [7].

2 A brief review of G/XFEM

The core concept of G/XFEM lies in enriching the Partition of Unity (PoU) framework with special functions tailored to capture the expected behavior of the solution. The PoU is defined as a collection of shape functions whose sum is equal to one at every point in the domain Ω. Another key notion in this context is the *cloud* (ω_α), which denotes the set of finite elements that share the node α and defines the local support for the enrichment associated with that node. The enrichment function set in G/XFEM is defined as:

$$I_\alpha \stackrel{def}{=} \{L_{\alpha 1}, L_{\alpha 2}, ..., L_{\alpha q_\alpha}\} = \{L_{\alpha i}\}_{i=1}^{q_\alpha} \qquad \text{with } L_{\alpha 1} = 1, \tag{1}$$

where I_α is a set composed of q_α functions $L_{\alpha i}$, defined for node α.

The G/XFEM shape functions are constructed by multiplying the original nodal shape functions by their corresponding enrichment functions:

$$\{\phi_{\alpha i}\}_{i=1}^{q_\alpha} = N_\alpha \{L_{\alpha i}\}_{i=1}^{q_\alpha} \qquad \text{(no summation over } \alpha), \tag{2}$$

where N_α is the original PoU shape function associated with node α.

Consequently, the general G/XFEM approximation $\tilde{u}(\boldsymbol{x})$ is expressed as:

$$\tilde{u}(\boldsymbol{x}) = \sum_{\alpha=1}^{NN} N_\alpha(\boldsymbol{x}) \left\{ u_\alpha + \sum_{i=2}^{q_\alpha} L_{\alpha i}(\boldsymbol{x}) b_{\alpha i} \right\}, \tag{3}$$

where NN is the total number of nodes, and u_α and $b_{\alpha i}$ are nodal degrees of freedom corresponding to the standard FEM and enriched components, respectively.

3 ZZ-BD error estimator

The ZZ-BD estimator [5] defines the recovered stress field as:

$$\boldsymbol{\sigma}^* = \begin{pmatrix} \sigma^*_{xx} \\ \sigma^*_{yy} \\ \sigma^*_{xy} \end{pmatrix} = \sum_{\beta=1}^{NN} N_\beta \begin{pmatrix} a^1_{\beta,0} \\ a^2_{\beta,0} \\ a^3_{\beta,0} \end{pmatrix} + \sum_{\beta \in I} \sum_{n=1}^{2} N_\beta \begin{pmatrix} a^1_{\beta,n} g^1_n(r,\theta) \\ a^2_{\beta,n} g^2_n(r,\theta) \\ a^3_{\beta,n} g^3_n(r,\theta) \end{pmatrix}, \tag{4}$$

where r and θ are polar coordinates centered at the crack tip, and I denotes the set of nodes enriched with singular functions g^d_n ($d = 1, 2, 3$ are stress components indexes and $n = 1, 2$ are the crack opening modes). These functions represent the asymptotic stress field contributions near the crack tip for modes I and II, as detailed in [5].

The coefficients $a^d_{\beta,n}$ in eq.(4) are nodal parameters obtained by minimizing a functional through a locally weighted L_2 projection, leading to the following system:

$$\tilde{\mathbf{A}}^d \, \tilde{\mathbf{a}}^d = \mathbf{f}^d \tag{5}$$

$$\tilde{A}^d_{(\alpha,m)(\beta,n)} = \begin{cases} 0, & \alpha \neq \beta \\ \left(g^d_n, g^d_m\right)^{N_\alpha}_{L_2(\omega_\alpha)}, & \alpha = \beta \end{cases} \tag{6}$$

$$\left(g^d_n, g^d_m\right)^{N_\alpha}_{L_2(\omega_\alpha)} = \int_{\omega_\alpha} g^d_n \, g^d_m \, N_\alpha \, d\Omega, \tag{7}$$

where $\tilde{\mathbf{a}}^d$ contains the nodal unknowns, $\tilde{\mathbf{A}}^d$ is a symmetric positive-definite block-diagonal matrix and node indices $\alpha, \beta = 1, ..., NN$, $m = 0, ..., NEF(\alpha)$ and $n = 0, ..., NEF(\beta)$, with NEF representing the number of enrichment functions of node α or β.

The block-diagonal nature of $\tilde{\mathbf{A}}^d$ enables much more efficient factorization than the global projections proposed in [8, 9].

4 Goal-oriented error estimator

4.1 Error in the quantity of interest

For a linear quantity of interest $Q(\boldsymbol{u})$ based on the approximate displacement field $\tilde{\boldsymbol{u}}$ obtained from a Galerkin Method approach, the exact error is defined as:

$$Q(\boldsymbol{u}) - Q(\tilde{\boldsymbol{u}}) = Q(\boldsymbol{u} - \tilde{\boldsymbol{u}}) = Q(\boldsymbol{e}). \tag{8}$$

An estimate of this error can be expressed in terms of the residual and an influence function $\boldsymbol{w}$ [10]:

$$Q(\boldsymbol{e}) = B(\boldsymbol{e}, \boldsymbol{w}), \tag{9}$$

where $B(\cdot, \cdot)$ is a bilinear form, and $\boldsymbol{w}$ is the solution of the so-called "dual problem", defined as:

$$B(\boldsymbol{v}, \boldsymbol{w}) = Q(\boldsymbol{v}), \quad \forall \boldsymbol{v} \in \mathscr{V}. \tag{10}$$

In eq. 10, $\mathscr{V}$ represents the space of admissible functions. For reference, the corresponding weak formulation of the primal boundary value problem – whose error is being estimated – is given by:

$$B(\boldsymbol{u}, \boldsymbol{v}) = l(\boldsymbol{v}), \qquad \forall\, \boldsymbol{v} \in \mathscr{V}. \tag{11}$$

The function $\boldsymbol{w}$ is commonly referred to as the influence function associated with Q, as it indicates how the residual affects the error in the quantity of interest [10].

Using the same approximation space $\tilde{\mathscr{V}}$ as the primal problem, an approximate solution $\tilde{\boldsymbol{w}}$ of the dual satisfies:

$$B(\tilde{\boldsymbol{v}}, \tilde{\boldsymbol{w}}) = Q(\tilde{\boldsymbol{v}}), \quad \forall \tilde{\boldsymbol{v}} \in \tilde{\mathscr{V}}. \tag{12}$$

The exact error in Q can then be computed from the primal and dual problems errors $\boldsymbol{e}$ and $\boldsymbol{e}^w$:

$$Q(\boldsymbol{e}) = B(\boldsymbol{e}, \boldsymbol{e}^w). \tag{13}$$

An **estimated error** for Q can be derived using energy norm estimators for primal and dual problems. When using recovery-based techniques, the following expression is derived:

$$Q(\boldsymbol{e}^*) = \int_\Omega (\boldsymbol{\sigma}^* - \tilde{\boldsymbol{\sigma}})^T \boldsymbol{C}^{-1} (\boldsymbol{\sigma}^{w*} - \tilde{\boldsymbol{\sigma}}^w)\, d\Omega, \tag{14}$$

where $\tilde{\boldsymbol{\sigma}}$ and $\tilde{\boldsymbol{\sigma}}^w$ are the approximate stress fields, and $\boldsymbol{\sigma}^*$ and $\boldsymbol{\sigma}^{w*}$ are the recovered stress fields for primal and dual problems computed by the ZZ-BD technique.

The error estimation is performed at the element level, with the resulting local contributions assembled to yield the global error defined in eq. 14:

$$Q(\boldsymbol{e}^*) = \sum_{k=1}^{NE} Q^k(\boldsymbol{e}^*), \tag{15}$$

$$Q^k(\boldsymbol{e}^*) = \int_{\Omega_k} (\boldsymbol{\sigma}^* - \tilde{\boldsymbol{\sigma}})^T \boldsymbol{D}^{-1} (\boldsymbol{\sigma}^{w*} - \tilde{\boldsymbol{\sigma}}^w)\, d\Omega_k, \tag{16}$$

where $Q^k(\boldsymbol{e}^*)$ denotes the estimated error in element k and NE is the total number of elements in the mesh.

4.2 Error estimator for the SIF

In this work, a goal-oriented estimator for the SIF is proposed using the Interaction Integral as extraction method. In the dual problem formulation, the term $Q(\tilde{\boldsymbol{v}})$ in eq. 12 is defined as:

$$Q(\tilde{\boldsymbol{v}}) = \frac{E^*}{2} \int_A \left[\tilde{\sigma}_{ij} \frac{\partial u_i^{(2)}}{\partial x_1} + \sigma_{ij}^{(2)} \frac{\partial \tilde{v}_i}{\partial x_1} - \tilde{\sigma}_{ij} \varepsilon_{ij}^{(2)} \delta_{1j} \right] \frac{\partial q}{\partial x_j} dA, \tag{17}$$

where superscript (2) denotes an auxiliary stress state from the first term of the asymptotic expansion (see [6]), A is the integration domain defined by a circle of radius r centered at the crack tip (Figure 1(a)) and q is a weight function that takes the value one at all nodes located within the circular domain of radius r, and zero at all other

nodes. Within each element, q is defined by the interpolation of its nodal values. As a result, the derivatives of q (appearing in eq. 17) are nonzero only in elements that contain at least one, but not all, nodes inside the circle associated with r, as illustrated in Fig. 1(b). Finally, the effective modulus E^* is E for plane stress and $\frac{E}{1-\nu^2}$ for plane strain.

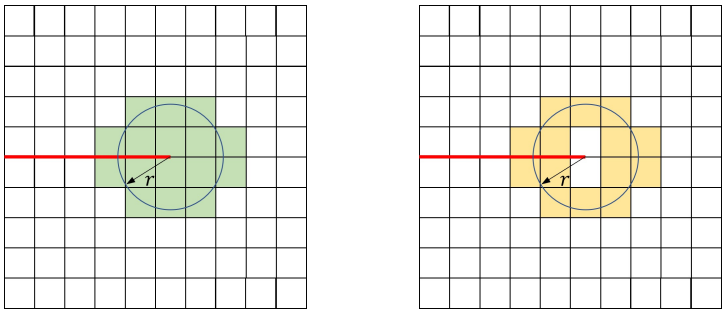


Figure 1. (a) Elements composing domain A (green).(b) Elements with nonzero derivatives of q (yellow).

Details on the interaction integral formulation and its use in the dual problem are given in [11]. The approximate dual solution $\tilde{\boldsymbol{w}}$ is computed by:

1. Assembling the dual stiffness matrix, reusing the primal stiffness matrix.
2. Computing the dual load vector by evaluating eq. 17 element-wise over domain A. For mixed-mode scenarios, separate load vectors for K_I and K_{II} are constructed from pure mode states.
3. Solving the dual system to obtain $\tilde{\boldsymbol{w}}$ nodal values.
4. Post-processing the dual solution to compute stresses and applying the ZZ-BD energy norm estimator.

Finally, the estimated SIF error is obtained from the recovered stresses of primal and dual problems by eq. 14.

5 Numerical Results

The proposed error estimator is evaluated using a plate with an edge crack (Fig. 2), where the exact stress solution is given by the asymptotic expansion of crack tip fields for modes I and II, imposed as Neumann boundary conditions. This allows exact computation of energy norm errors and estimator effectivities.

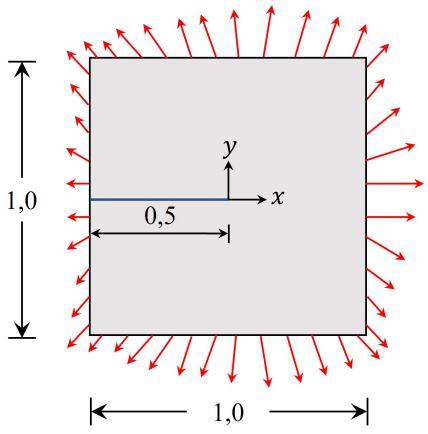
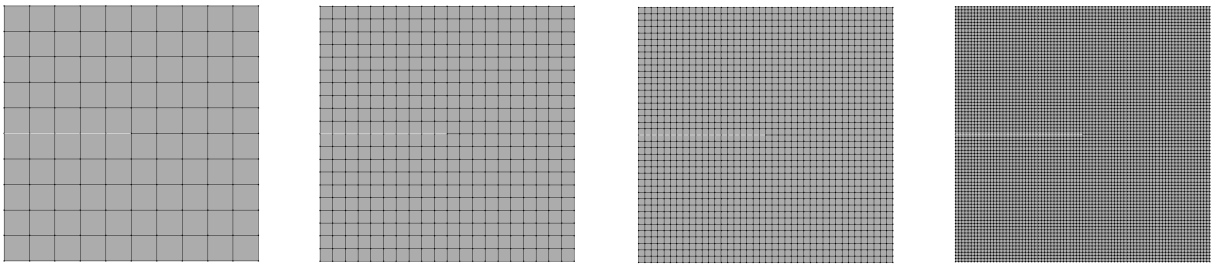


Figure 2. Problem A: plate with edge crack, exact solution imposed as Neumann boundary conditions.

A mixed-mode loading is considered on four nested meshes of Q4 elements, shown in Fig. 3, following the validation setup of Lins et al. [5] for the ZZ-BD estimator. The geometric enrichment strategy employs OD branch functions [12], which are assigned to all nodes within a 0.25×0.25 region centered at the crack tip, as well as to nodes located along the crack path and in the immediate layers above and below it. Only OD branch functions were adopted for enrichment, ensuring consistency with the original ZZ-BD framework [5], which did not include Heaviside functions along the crack path. The enriched nodes on the 20×20 mesh are depicted in Fig. 4.



(a) (b) (c) (d)

Figure 3. Mesh sequence for goal-oriented error estimator study: (a) 10×10, (b) 20×20, (c) 40×40, (d) 80×80.

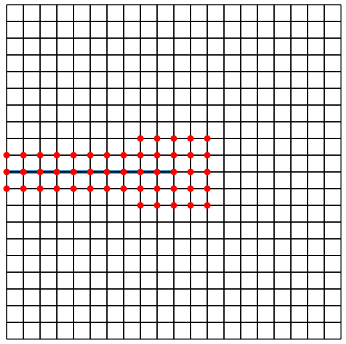


Figure 4. Nodes enriched with singular functions (red) in the 20×20 mesh; crack shown in blue.

The radius r defining the integration domain A in the Interaction Integral influences the SIF estimate and dual problem load. Elements contribute only if intersected by the circle of radius r but not entirely inside it (where derivatives of q vanish). Figure 1(b) illustrates this condition. The radii used are $r = 3h$ for 10×10, $r = 6h$ for 20×20, $r = 12h$ for 40×40, and $r = 24h$ for 80×80 meshes.

The following metrics assess the estimator:

- Exact errors $\mathscr{E}(K_1)$ and $\mathscr{E}(K_2)$ for K_I and K_{II}, computed from exact values $K_I = K_{II} = \sqrt{2\pi}$.
- Estimated errors $\mathscr{E}^*(K_1)$ and $\mathscr{E}^*(K_2)$ using the proposed estimator (eq. 14).
- Effectivity indices θ^{K_1} and θ^{K_2}, defined as:

$$\theta^{K_i} = \frac{\mathscr{E}^*(K_i)}{\mathscr{E}(K_i)}, \quad i = 1, 2 \tag{18}$$

Figure 5 displays the exact and estimated errors for K_I and K_{II} as functions of the number of degrees of freedom (DOF). The results reveal a close agreement between the estimated and exact errors across all mesh levels, with the difference decreasing as the mesh is refined. This trend highlights the accuracy and robustness of the proposed goal-oriented estimator.

Figure 6 presents the effectivity indices for the proposed estimator applied to both K_I and K_{II}. The indices are generally close to the ideal value of unity, particularly for the finer meshes, indicating a high level of accuracy in the estimated error. A noticeable deviation occurs for the coarsest mesh (10×10), where the limited resolution leads to reduced estimator performance. This behavior is expected, as the estimator relies on accurate representations of both the primal and dual solutions. Additionally, because the goal-oriented estimator involves the product of two independent energy norm error estimates, its effectivity values tend to deviate more from unity than those of estimators applied solely to the primal problem. Nevertheless, the observed trend with mesh refinement demonstrates consistent improvement and convergence toward ideal effectivities, reinforcing the reliability of the proposed approach.

Figure 7 shows element-wise estimated errors for the 40×40 mesh. The estimated error in the dual problem is concentrated around the region where the loads are applied (corresponding to the interaction integral domain (Fig. 1(b))). In contrast, the primal error is primarily localized near the crack tip, where the singularity occurs. Consequently, the estimated error in K_I reflects the combined effect of these two localized regions, as it results from the product of the primal and dual error distributions.

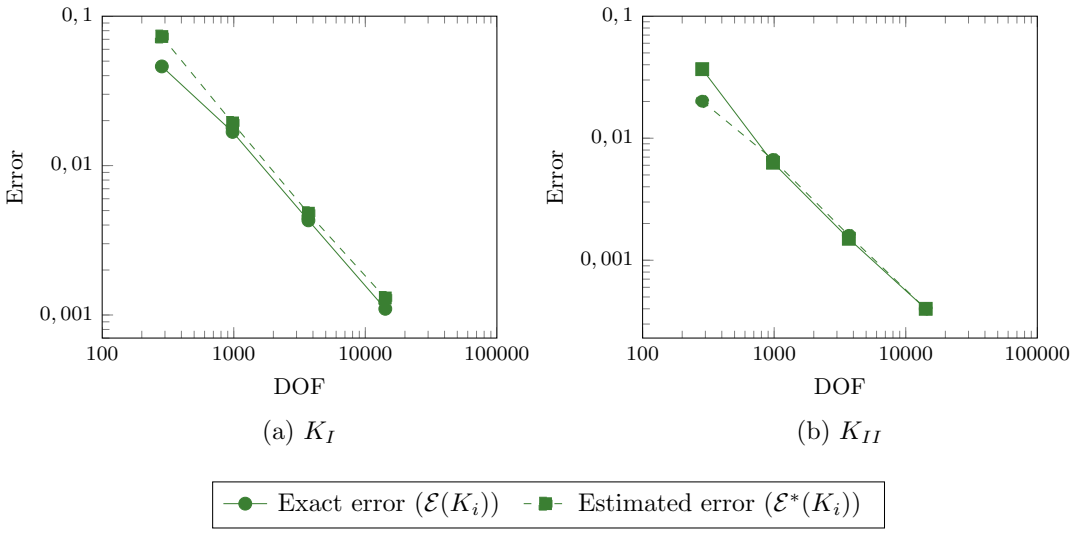


Figure 5. Exact and estimated SIF errors for K_I and K_{II}, logarithmic scales.

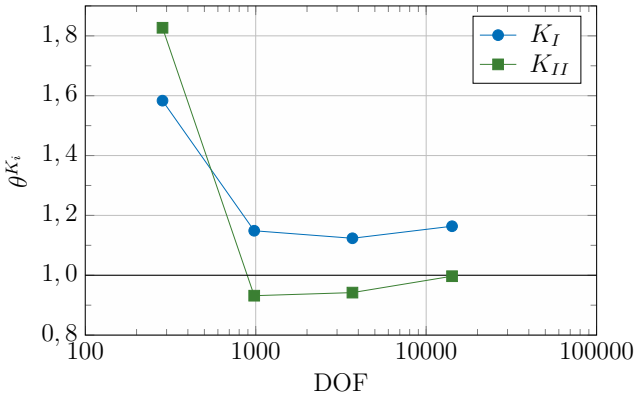


Figure 6. Effectivity indices for the SIF estimator; x axis logarithmic.

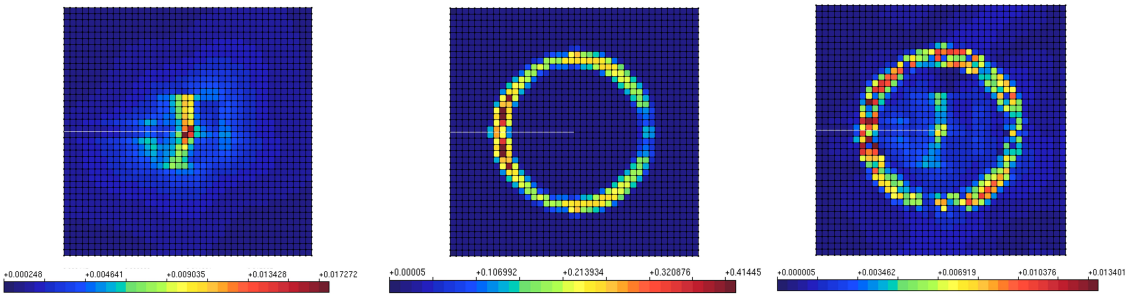


Figure 7. Element-wise estimated errors for the 40×40 mesh, $r = 12h$: (a) primal problem, (b) dual problem, (c) error in K_I.

6 Conclusions

This work presented a goal-oriented error estimator specifically designed for the SIF within the G/XFEM framework. The proposed estimator is based on the Interaction Integral method to formulate the dual problem related to the quantity of interest, combined with the ZZ-BD recovery technique to estimate the errors in both primal and dual problems. This approach allows for an accurate estimation of the error directly associated with the SIF, which is a fundamental parameter in fracture mechanics.

The numerical experiments performed on a two-dimensional mixed-mode crack problem demonstrated the effectiveness of the estimator. The estimated errors closely matched the exact errors, and the effectivity indices

remained near unity for most mesh refinements, validating the accuracy and robustness of the method. The results also highlighted the influence of mesh quality, with the coarsest mesh yielding slightly less accurate estimates.

In addition to providing reliable global error estimates for the SIF, the proposed estimator offers detailed local error distributions in both primal and dual problems, which can guide adaptive mesh refinement strategies to improve solution accuracy in critical regions. Future research may extend the present methodology to three-dimensional settings, more complex crack geometries, and automated adaptive frameworks to further enhance its applicability and efficiency.

References

[1] T. Belytschko, R. Gracie, and G. Ventura. A review of extended/generalized finite element methods for material modeling. *Modelling and Simulation in Materials Science and Engineering*, vol. 17, n. 4, pp. 043001, 2009.

[2] C. Duarte, I. Babuška, and J. Oden. Generalized finite element methods for three-dimensional structural mechanics problems. *Computers & Structures*, vol. 77, n. 2, pp. 215–232, 2000.

[3] T. Strouboulis, I. Babuška, and K. Copps. The design and analysis of the generalized finite element method. *Computer Methods in Applied Mechanics and Engineering*, vol. 181, n. 1-3, pp. 43–69, 2000.

[4] G. M. Fonseca, F. B. Barros, and R. M. Lins. An a posteriori error estimator for the generalized finite element method with global-local enrichments in fracture mechanics. *International Journal for Numerical Methods in Engineering*, vol. 126, n. 13, pp. e70079, 2025.

[5] R. Lins, S. P. Proença, and C. A. Duarte. Efficient and accurate stress recovery procedure and a posteriori error estimator for the stable generalized/extended finite element method. *International Journal for Numerical Methods in Engineering*, vol. 21, 2019.

[6] N. Moes, J. Dolbow, and T. Belytschko. A finite element method for crack growth without remeshing. *International Journal for Numerical Methods in Engineering*, vol. 46, n. 1, pp. 131–150, 1999.

[7] F. T. Fonseca and R. L. Pitangueira. An object oriented class organization for dynamic geometrically non-linear. In *Proceedings of CILAMCE(Iberian-Latin-American Congress on Computational Methods in Engineering)*, 2007.

[8] R. M. Lins, M. D. C. Ferreira, S. P. B. Proença, and C. A. Duarte. An a-posteriori error estimator for linear elastic fracture mechanics using the stable generalized/extended finite element method. *Computational Mechanics*, vol. 56, n. 6, pp. 947–965, 2015.

[9] C. Prange, S. Loehnert, and P. Wriggers. Error estimation for crack simulations using the XFEM. *International Journal for Numerical Methods in Engineering*, vol. 91, n. 13, pp. 1459–1474, 2012.

[10] J. Oden and S. Prudhomme. Goal-oriented error estimation and adaptivity for the finite element method. *Computers & Mathematics with Applications*, vol. 41, n. 5-6, pp. 735–756, 2001.

[11] G. M. Fonseca. *Estimadores de erro a posteriori e Estratégias Adaptativas para o Método dos Elementos Finitos Generalizados com Enriquecimento Global-local Aplicado a Problemas da Mecânica da Fratura*. PhD thesis, Universidade Federal de Minas Gerais, Belo Horizonte, MG, Brasil, 2023.

[12] J. T. Oden and C. A. Duarte. Clouds, cracks and FEM's. In *Recent Developments in Computational and Applied Mechanics:A Volume in Honour of John B Martin. Barcelona: CIMNE*, 1997.